Evidence for Sequential Two-Body Decay in Three-Body Decay of C^{12} and B^{10}†

E. H. Beckner, C. M. Jones, and G. C. Phillips
Rice University, Houston, Texas
(Received February 27, 1961)

The reactions $B^{11}(p,\alpha)Be^8$ and $Be^9(p,d)Be^8$ have been studied by employing monoenergetic protons, thin targets, and a low-background magnetic spectrometer to resolve the disintegration products. The continuum spectra of alpha and deuteron particles produced, respectively, in the reactions have been compared to the generalized density-of-states function of Phillips, Griffy, and Biedenharn and good fits have been obtained. The density function was calculated from the experimental (α,α) scattering phase shifts. The calculated S-wave density function for Be^8 predicts a low-energy anomaly. This anomaly has been observed and confirms the assumption of the model used to calculate this spectral shape: three-body decay proceeding *via* a sequence of two-body decay modes.

INTRODUCTION

THE cluster model suggests that three-body nuclear decay can be treated as a time sequence of two-body interactions.[1] A consideration of the three-body decay reaction

$$a+A \rightarrow D^* \rightarrow b+C+c,$$

as a sequence of two-body decays

$$D^* \rightarrow B^*+b, \quad B^* \rightarrow C+c,$$

has been shown to allow predictions about the cross section for emission of particles b.[2] In particular, if B^* is produced in a localized state of radius a and possesses only one channel for decay, $c+C$, whose scattering phase shift δ_l is shown, then the cross section for emission of particles b is determined largely by the density-of-states function,

$$\rho=\frac{1}{\pi}\frac{d}{dE}[\delta_l(E_B)+\phi_l(E_B,a)], \tag{1}$$

where $\phi_l \equiv \tan^{-1}(F_l/G_l)$ is a "hard sphere" phase shift. The assumption that the reaction

$$a+A \rightarrow D^* \rightarrow b+C+c$$

can be treated as a sequence of two-body decays requires the decay of D^* to occur in such a manner that the constituents of B^*, $c+C$, remain inside the small volume determined by the interaction radius a for a time at least slightly longer than that required for the emission of particle b. The excited, localized, system B^* then decays into $c+C$. This mechanism effectively assumes that there is spatial localization in the production of the system B^*. Under these conditions it is possible to write[2] the complete expression for the cross section for emission of particles b:

$$\sigma_l(E_B)=\rho_l(E_B) \times\left\{\frac{\mu_a\mu_b}{4\pi^2\hbar^4}\left(\frac{k_b}{k_a}\right)|\langle B+b, E_B|H'|A+a, E_A\rangle|^2\right\}, \tag{2}$$

where

$$\rho_l(E_B)=\sum_n \delta(E_B-E_n)+\frac{1}{\pi}\frac{d}{dE_B}[\delta_l(E_B)+\phi_l(E_B,a)], \tag{3}$$

with $\sum_n \delta(E_B-E_n)$ as the term which completely determines $\rho_l(E_B)$ if B contains only a set of sharp states at E_n. Here $\delta_l(E_B)$ is the phase shift for the reaction

$$c+C \rightarrow B^* \rightarrow c+C,$$

and

$$\phi_l(E_B,a)=\tan^{-1}(F_l/G_l)\,|_{R=a}. \tag{4}$$

H' is the interaction Hamiltonian for

$$a+A \rightarrow D^* \rightarrow b+B^*,$$

and $|a+A, E_A\rangle$ is the initial state vector and $|b+B, E_B\rangle$ is the final state vector. It should be noted that a somewhat different form of the generalized density-of-states function $\rho_l(E_B)$ was also obtained by Phillips *et al.*[2] when a renormalization of the final state wave function was employed. The form of the function given in Eqs. (1) and (3) was obtained by extending the method normally employed for discrete bound states[3] to include the continuum states by treating these latter states as discrete.

This paper will compare these predictions to experiment for the formation of the nuclear system Be^8 by deuteron and alpha decay of B^{10*} and C^{12*}, respectively.

Two reactions leading to Be^{8*} have been studied in an effort to explore the predictions of this density-of-states function: $Be^9(p,d)Be^{8*}$ and $B^{11}(p,\alpha)Be^{8*}$. Thus for the first reaction the sequential decays considered are

$$Be^9+p \rightarrow B^{10*} \rightarrow Be^8+d,$$

and then

$$Be^{8*} \rightarrow \alpha+\alpha.$$

For the second reaction the sequence of events considered is

$$B^{11}+p \rightarrow C^{12*} \rightarrow \alpha+Be^{8*},$$

† Supported by the U. S. Atomic Energy Commission.

[1] G. C. Phillips and T. A. Tombrello, Nuclear Phys. **19**, 525 (1960).

[2] G. C. Phillips, T. A. Griffy, and L. C. Biedenharn, Nuclear Phys. **21**, 327 (1960). G. C. Phillips and L. C. Biedenharn, Bull. Am. Phys. Soc. **5**, 44 (1960).

[3] L. I. Schiff, *Quantum Mechanics* (McGraw-Hill Book Company, Inc., New York, 1949), p. 195.

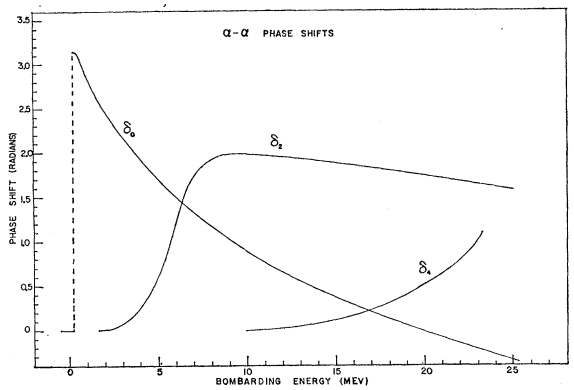

FIG. 1. The experimental $\alpha-\alpha$ scattering phase shifts summarized by Jones *et al.*[4] which were employed to develop the density-of-states function $\rho(E_{\mathrm{Be}^8})$.

and then

$$\mathrm{Be}^{8*} \rightarrow \alpha+\alpha.$$

For both reactions the work by Jones *et al.*[4] on $\alpha-\alpha$ scattering provided the necessary information about the phase shifts δ_l for the calculation of $\rho_l(E_{\mathrm{Be}^8})$. The Rice University Van de Graaff accelerator provided the bombarding protons for these studies while the Rice University 180° magnetic spectrometer served as detector of the decay particles.[5] Photographic plates were used in the spectrometer for these experiments. This permitted a careful study to be made of the energy regions possessing low cross sections. The targets employed were thin, self-supporting Be foils for the Be^9 experiment and enriched B^{11} evaporated on thin carbon foils for the B^{11} experiment. In both experiments the target thickness was approximately 65 kev for the (p,α) or (p,d) reaction forming the ground state of Be^8.

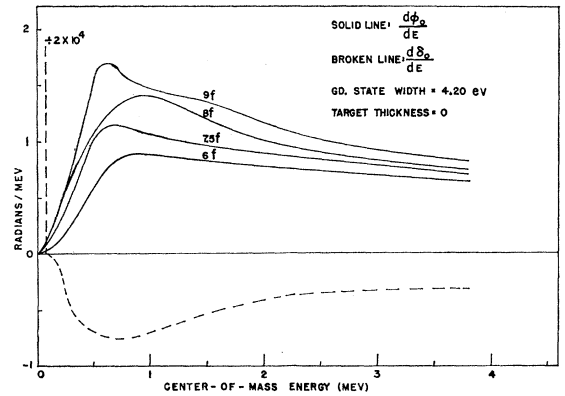

FIG. 2. $d\delta_0/dE$ and $d\phi_0/dE$ for various a, as a function of $\alpha-\alpha$ center-of-mass energy, where $\phi_0=\tan^{-1}(F_0/G_0)\,|_{R=a}$ and $\delta_0=S$-wave $\alpha-\alpha$ scattering phase shift.

[4] C. M. Jones, G. C. Phillips, and P. D. Miller, Phys. Rev. **117**, 525 (1960).

[5] K. F. Famularo and G. C. Phillips, Phys. Rev. **91**, 1195 (1953).

DEVELOPMENT OF THE PREDICTED SPECTRAL DISTRIBUTIONS

The $\alpha-\alpha$ phase shifts summarized by Jones *et al.*[4] are shown in Fig. 1. These consist of the work of Heydenburg and Temmer[6] for incident alpha energies of $0<E_\alpha\leqslant 3$ Mev, Russell *et al.*[7] for $3\leqslant E_\alpha\leqslant 5.9$ Mev, Jones *et al.*[4] for $5\leqslant E_\alpha\leqslant 9$ Mev, and Nilson *et al.*[8] for $12\leqslant E_\alpha\leqslant 20$ Mev. The resulting $d\delta_0/dE$ curve is shown in Fig. 2 along with $d\phi_0/dE$ for various radii a. Figure 3 shows the sum of these two functions for various a. Since the density-of-states function is required to be positive, it is seen that certain radii must be excluded from consideration in selecting the most suitable radius for the reactions. A surprising anomaly is seen to be present in the energy region of about 0.5 to 1.0 Mev. The relative intensity of this anomaly to the ground-state group, and to a certain extent the shape of the anomaly, are determined solely by the radius of interaction a selected as appropriate. However, it is seen that any

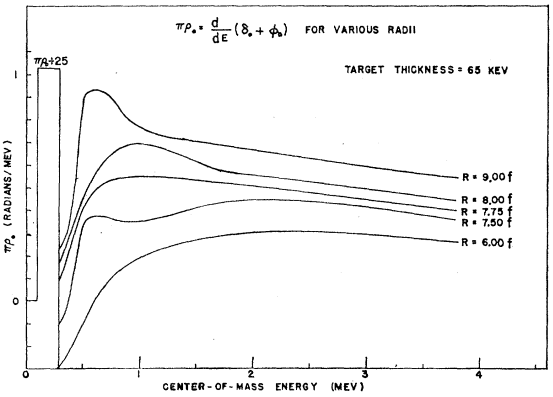

FIG. 3. Predicted S-wave spectral distributions, for various a, leading to low excitations of Be^8. The calculated curve has been averaged over a 65-kev target thickness.

radius generates the anomaly. It should also be noted that the radius a used in Eqs. (2)–(4) is *not* the same radius which one derives from $\alpha-\alpha$ scattering: a is defined as describing the interaction volume of the system Be^{8*}+produced particle.

In a similar way the Be^8 D-wave states may be calculated. Figure 4 shows the curves $d\delta_2/dE$ and $d\phi_2/dE$ for various radii. Figure 5 shows the sum $\pi\rho_2=d\delta_2/dE+d\phi_2/dE$. In developing the complete expression for $\pi\rho_l(E_B)$ no consideration was given to the next higher term, $\pi\rho_4=(d/dE)(\delta_4+\phi_4)$, since it is much smaller than either $\pi\rho_0$ or $\pi\rho_2$: in fact δ_4 only begins to become noticeable at about $E_\alpha=10$ Mev.

It is also necessary to account for a very undesirable

[6] N. P. Heydenburg and G. M. Temmer, Phys. Rev. **104**, 123 (1956).

[7] J. L. Russell, Jr., G. C. Phillips, and C. W. Reich, Phys. Rev. **104**, 135 (1956).

[8] R. Nilson, W. K. Jentschke, G. R. Briggs, R. O. Kerman, and J. N. Snyder, Phys. Rev. **109**, 850 (1958).

feature of this type of reaction. In the case of $B^{11}+p \rightarrow C^{12*} \rightarrow Be^{8*}+\alpha_0$ and the subsequent decay $Be^{8*} \rightarrow \alpha_1+\alpha_2$, it is seen that the end, detected, result is merely the three alpha particles α_0, α_1, and α_2. Unfortunately these three particles are indistinguishable when detected on the photographic plate and the experimental alpha spectrum contains all three types of particles. The preceding calculations determine only the spectral distribution of α_0, so it is necessary to calculate the contribution of $\alpha_1+\alpha_2$ in order to fit the experimental data. A similar situation is seen to exist for $Be^9+p \rightarrow B^{10*} \rightarrow Be^{8*}+d_0$, with subsequent decay $Be^{8*} \rightarrow \alpha+\alpha$. In this case it is possible for B^{10*} to decay via: $B^{10*} \rightarrow Li^{6*}+\alpha$ and then $Li^{6*} \rightarrow \alpha+d_1$. It is thus necessary to include the contribution of both d_0 and d_1 when attempting to fit the theory to the experimental deuteron spectrum. The calculations of these effects are discussed in the Appendix.

For the $B^{11}(p,\alpha)Be^8$ reaction leading to D states in Be^8, Fig. 6 shows the results of the calculations. In

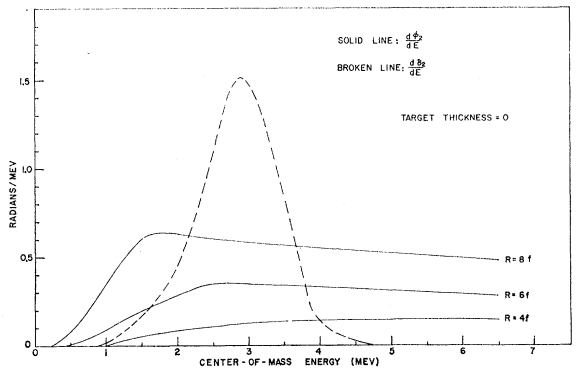

FIG. 4. $d\delta_2/dE$ and $d\phi_2/dE$ for various a, as a function of $\alpha-\alpha$ center-of-mass energy, where $\phi_2=\tan^{-1}(F_2/G_2)\,|_{R=a}$ and $\delta_2=D$-wave $\alpha-\alpha$ scattering phase shift.

Fig. 6 are plotted two functions and their sum: the function $N_{1,2}$ is represented by the curve labeled *breakup alphas* produced by the decay of Be^{8*}, while the function N_0 is shown as the predicted yield of *initial* α_0 particles emitted from the $B^{11}(p,\alpha_0)Be^{8*}$ reaction. The total number of particles of type $\alpha_{1,2}$ is, of course, twice as great as the number of α_0 particles. The function $\pi\bar{\rho}_2$ was assumed to consist only of the term

$$\pi\rho_2 P=\frac{d}{dE}(\delta_2+\phi_2)P\bigg|_{R=4f},$$

where P is the penetrability factor for the α emission under consideration. This curve neglects contributions to the breakup spectrum due to $\bar{\rho}_0$ and $\bar{\rho}_4$ whose yields are small in the region of interest.

A similar calculation was made for $Be^9(p,d_0)Be^{8*}$ to determine the contribution of the reaction $Be^9(p,\alpha)Li^{6*}$,

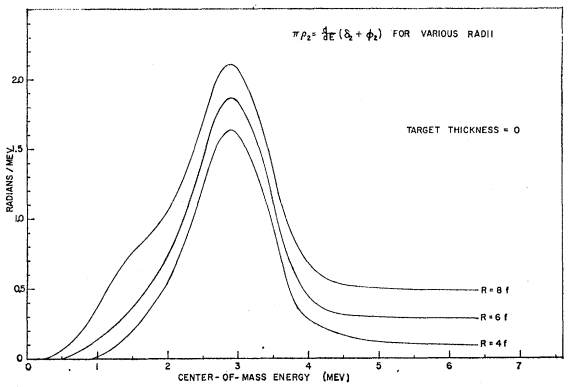

FIG. 5. Predicted D-wave spectral distribution, for various a.

$Li^{6*} \rightarrow \alpha+d_1$. The data of Browne and Bockelman[9] and Browne *et al.*[10] were used to compare the cross section for formation of Li^{6*} with that for $Be^8(0)$. It was only possible to get an approximate comparison due to differences in bombarding energy and angle of detection. The value assumed was $\sigma[Be^8(0)]/\sigma(Li^{6*})=10$, for Li^6 excited to 2.184 Mev. In order to obtain deuterons d_1 of the same energies as those of d_0, the only allowed levels of excitation in Li^6 were 2.184, 3.560, and 4.520 Mev. The only large contribution results from the level at 2.184 Mev in Li^6, since the 3.56 level has been found to emit γ rays rather than deuterons[11] and the 4.52 level is very broad and weak.[9] The 2.184 deuterons contribute approximately 20% to the deuteron spectrum shown in Fig. 10 in the region $2.5<E_x<3.5$ Mev. Consequently the fit to the data in this region is quite dependent on the value taken for $\sigma[Be^8(0)]/\sigma[Li^6(2.184)]$.

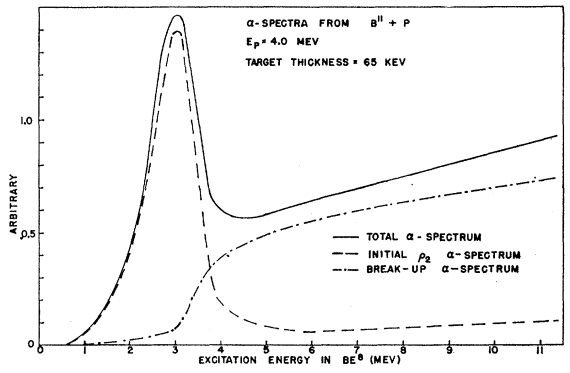

FIG. 6. Predicted Be^8 D states spectra from $B^{11}+p$. The α_0 spectrum from $B^{11}(p,\alpha_0)Be^{8*}$ is assumed to be represented in this energy region by $\pi\bar{\rho}_2$ only. The breakup $\alpha_{1,2}$ spectrum results from the spectral distribution predicted by $\pi\bar{\rho}_2$ for the formation of Be^{8*}. The α_0 have been assumed to be emitted with $l=1$; however, penetrability effects change the spectral shape very little. The radius a was 4×10^{-13} cm.

[9] C. P. Browne and C. K. Bockelman, Phys. Rev. **105**, 1304 (1957).
[10] C. P. Browne, R. M. Williamson, D. S. Craig, and D. J. Donahue, Phys. Rev. **83**, 179 (1951).
[11] F. Ajzenberg-Selove and T. Lauritsen, Nuclear Phys. **11**, 1 (1959).

COMPARISON OF THEORY WITH EXPERIMENTS

The $B^{11}(p,\alpha)Be^8$ Experiment

This experiment was performed at bombarding energies of 3.025, 4.025, and 5.009 Mev, and the corresponding α-particle spectra are shown in Figs. 7–9. The targets employed were enriched B^{11} evaporated on C^{12} foils, with target thickness of 65 kev. The anomaly in the region $E_x \sim 0.75$ Mev referred to previously is best seen in the 4.025-Mev spectrum. This bombarding energy proved to yield the largest cross section for emission to the ground state of Be^8, and consequently exhibits the largest anomaly. The theoretical curve was normalized to the height of the ground state, and was then used to predict the height of the curve for excitation energies in Be^8 of $0 \leqslant E_x \leqslant 1$ Mev.

Since the value of $|\langle B+b, E_B|H'|A+a, E_A\rangle|^2$ was not known for these reactions, it was necessary to introduce a constant κ to represent this term in Eq. (2):

$$\sigma = \frac{\mu_a \mu_b}{4\pi^2 \hbar^4}\left(\frac{k_b}{k_a}\right)[\kappa_0\rho_0 + \kappa_2\rho_2 + \kappa_4\rho_4],$$

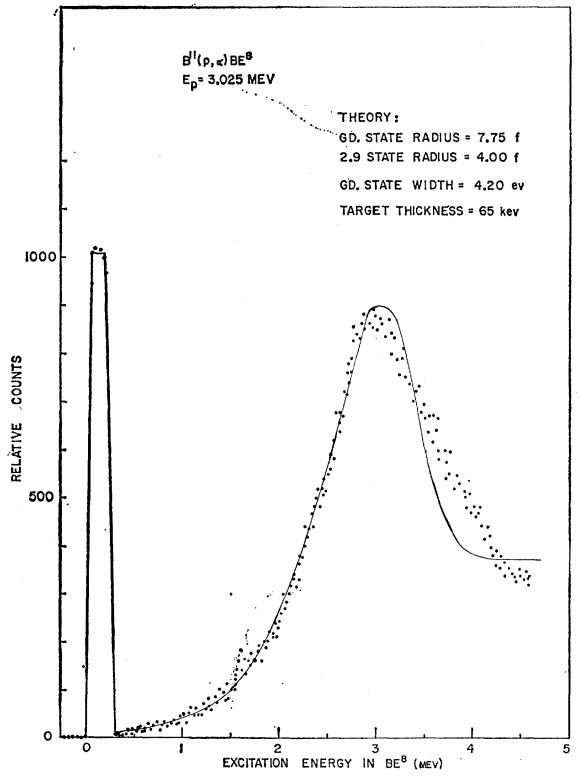

FIG. 7. Alpha-particle spectrum resulting from $B^{11}+p$, with $E_p=3.025$ Mev. The solid line is a theoretical fit with $\kappa_0/\kappa_2 = 0.0765$. The D-state spectrum is as shown in Fig. 6. Contributions to the breakup spectrum from S states in Be^8 have been neglected since they do not produce a significant number of alpha particles of the energy of interest. The S-state spectrum is as in Fig. 3 for 7.75 f, but includes a penetration factor for $l=1$ emission of the α_0 particles. The latter factor changes the spectral shape very little.

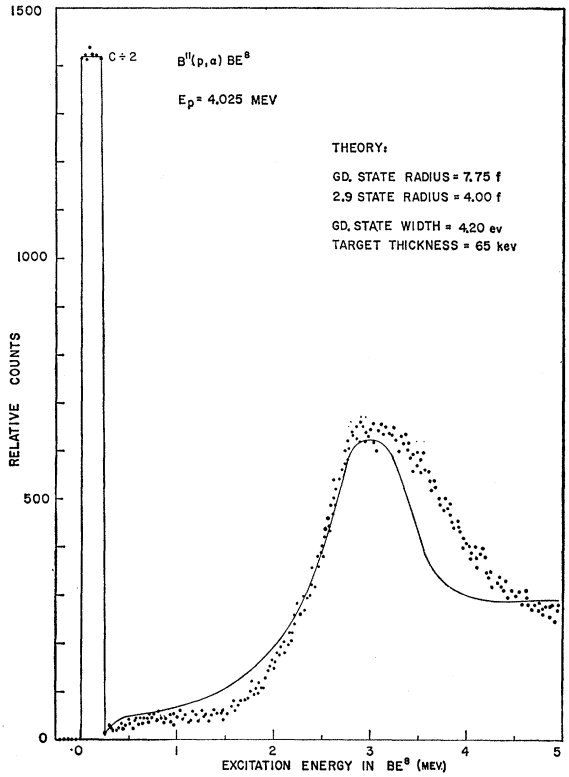

FIG. 8. Alpha-particle spectrum resulting from $B^{11}+p$, with $E_p=4.025$ Mev. The solid line is a theoretical fit with $\kappa_0/\kappa_2=0.294$. See caption for Fig. 7.

where κ_0 = value of $|\langle B+b, E_B|H'|A+a, E_A\rangle|^2$ for emission to the ground state of Be^8 for E_p being considered, κ_2 = value of $|\langle B+b, E_B|H'|A+a, E_A\rangle|^2$ for emission to the D state of Be^8, and with κ^4 assumed negligible for the region of interest. No interference terms have been included in the calculation. It was found that the best fit to the data could be made with:

$E_p=3.025$ Mev, $\kappa_0/\kappa_2=0.0765$;
$E_p=4.025$ Mev, $\kappa_0/\kappa_2=0.294$;
$E_p=5.009$ Mev, $\kappa_0/\kappa_2=0.0225$.

The $Be^9(p,d)Be^8$ Experiment

This experiment was performed with $E_p=5.205$ Mev and employed a self-supporting Be^9 foil. It was necessary to use the highest reasonable bombarding energy because of the low Q value of the reaction. Consequently, only the spectrum of Fig. 10 was obtained. This reaction clearly demonstrates the presence of an anomaly located in the region of $E_x \sim 0.75$ Mev. The ground-state group of deuterons was quite intense relative to the group leading to the 2^+ excited state of Be^8. This fact resulted in a substantial number of deuterons emitted into the region of the anomaly. The best fit was made to this data with the ratio $\kappa_0/\kappa_2=2.225$.

INTENSITIES OF THE Be^8 GROUND-STATE GROUP AND THE LOW-ENERGY ANOMALY

It is of interest to compare the intensities with which the ground state of Be^8 and the low-energy anomaly are populated. Three points are of importance: (1) the D and G wave states in Be^8 cannot account for this low-energy anomaly; (2) purely three-body decay mechanism cannot account for the anomaly (see below); (3) the generalized density-of-states function *can* account for an anomaly in Be^8 excitations to S states at about 0.75 Mev (see Figs. 2 and 3). In addition the density function predicts the ratio of ground-state intensity to the low-energy anomaly. This ratio is predicted to be about $(25/0.55)=45$ (see Fig. 3) for a 65-kev target and a radius of 7.75×10^{-13} cm. The experimental values, taken from Figs. 7–10 are $\leqslant 40$, $\leqslant 70$, $\leqslant 60$, and $\leqslant 60$, respectively. The fact that these experimental ratios are in reasonable agreement to the calculated one lends additional credence to the assumed sequential mechanism.

INVESTIGATION OF THREE-BODY EMISSION EFFECTS

An investigation has been made of the possibility of accounting for the spectral anomaly found in the region of 0.75 Mev in Be^8 on the basis of a purely three-body emission mechanism.[12] The calculation which was made was similar to those of Welton[13] and Uhlenbeck and Goudsmit.[14] The general approach taken in these calculations is to assume that the energy distribution of the three particles derives from the probability of a particular distribution being proportional to the corresponding volume in phase space. The familiar result is

$$f(\epsilon_3)d\epsilon_3=N(\epsilon_3)^{\frac{1}{2}}\left[E-\frac{m_1+m_2+m_3}{m_1+m_2}\epsilon_3\right]^{\frac{1}{2}}d\epsilon_3,$$

where $f(\epsilon_3)$ is the energy distribution for particle 3 of mass m_3. E is the total energy available to the three particles m_1, m_2, m_3, and ϵ_n is the energy of particle n. N is merely a normalizing factor. The predicted energy distribution for $B^{11}+p\rightarrow\alpha+\alpha+\alpha$, with $E_p=4.0$ Mev, is shown in Fig. 11. This figure shows the function $f(\epsilon_3)$ plotted as a function of excitation in Be^8.

It is necessary to include Coulomb barrier effects

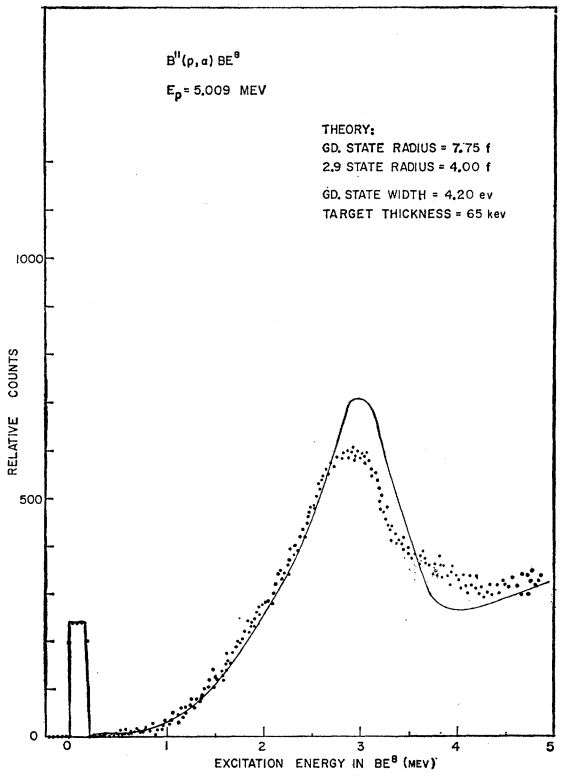

FIG. 9. Alpha particle spectrum resulting from $B^{11}+p$, with $E_p=5.009$ Mev. The solid line is a theoretical fit with $\kappa_0/\kappa_2=0.0225$. See caption for Fig. 7.

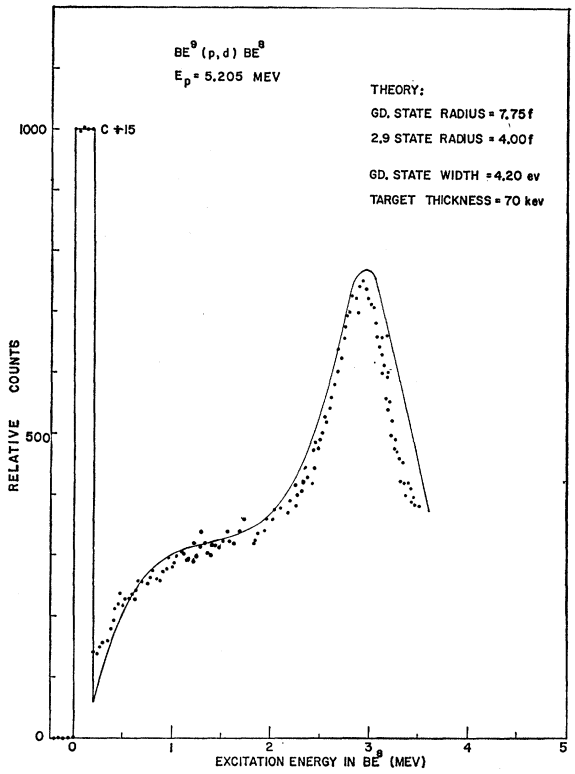

FIG. 10. Deuteron spectrum resulting from Be^9+p, with $E_p=5.205$ Mev. The solid line is a theoretical fit with $\kappa_0/\kappa_2=2.225$. The S and D states in Be^8 have been assumed to be formed by D- and S-wave deuteron emissions, respectively. These factors distort the spectral shape especially for large excitation energy in Be^8; however, they could not produce the anomaly at about 0.75 Mev.

[12] We wish to thank Dr. Robert B. Day for suggesting this analysis.

[13] T. A. Welton, private set of notes distributed by C. D. Moak.

[14] G. E. Uhlenbeck and S. Goudsmit, *Verhandelingen van Dr. P. Zeeman* (Martimus Nijhoff, The Hague, Netherlands, 1935), pp. 201–211.

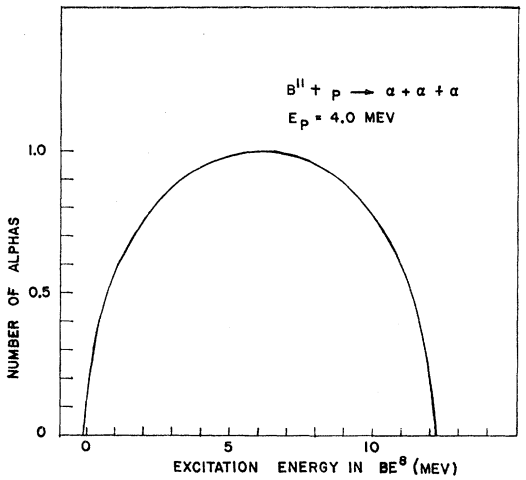

FIG. 11. Spectral distribution for $B^{11}+p\rightarrow\alpha+\alpha+\alpha$, $E_p=4.0$ Mev, when the distribution is assumed to depend only upon the phase-space volumes. The predicted distribution is shown as a function of the excitation energy in Be^8 which would result from the emission of alpha particles of the same energies as the breakup alphas but originating in the $B^{11}(p,\alpha)Be^8$ reaction.

on this energy distribution. The three emitted alpha particles must all penetrate the barrier with a given set of energies. Consequently, the probability of m_1, m_2, and m_3 being emitted with energies ϵ_1, ϵ_2, and ϵ_3 is determined by the product of the three corresponding penetrabilities $P_l^{(1)}P_l^{(2)}P_l^{(3)}$ and the distribution function determined by the usual phase-space volumes. The exact calculation of this distribution function has not been attempted. Rather, the simpler energy distribution

$$\lambda_n\equiv Nf(\epsilon_n)P_l^{(1)}P_l^{(2)}P_l^{(3)},$$

has been calculated. This function should exemplify the general nature of the three-body distribution function. The assumption was made that for a given energy ϵ_1 the particles 2 and 3 obtained equal energies, $\epsilon_2=\epsilon_3$. The results of this calculation are shown in Fig. 12, for $R=4$F and $R=8$F, with $l=0$ emission assumed for all three particles. A similar calculation was made for the case $\epsilon_2=3\epsilon_3$ rather than $\epsilon_2=\epsilon_3$. These results are also shown in Fig. 12 for $l=0$ and $R=8$F. It is seen that the shape of the distribution is almost independent of the manner in which particles 2 and 3 share the energy $E-\epsilon_1$.

These calculations show that the three-body emission mechanism is totally incapable of explaining the spectral anomaly at $E_x\approx0.75$ Mev in Be^8. The alpha particles being emitted to this region must possess almost all of the energy present in the compound system; consequently, if these particles are to originate from a three-body emission then the other two alpha particles can possess only very small energies. This requires that the penetrabilities for particles 2 and 3 be so small that the probability of this event occurring is quite small.

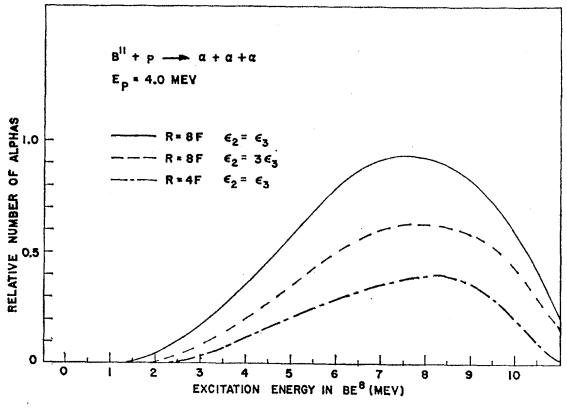

FIG. 12. Predicted spectral distribution from $B^{11}+p\rightarrow\alpha+\alpha+\alpha$ when Coulomb effects are superimposed on the distribution shown in Fig. 11. F≡fermi≡10^{-13} cm. (See text.)

CONCLUSIONS

The fit to the experiments shown in Figs. 7–10 seems to give good evidence for the validity of the approach taken by Phillips *et al.*, in the treatment of three-body decay.[2] Certainly, the spectral anomaly predicted for the region $E_x\sim0.75$ Mev is present and indicates the importance of spatial localization in the production of B* (here Be^{8*}).

Several investigations were made to determine that there could be no other source of these particles. Figure 13 shows a spectrum made for the reaction $F^{19}(p,\alpha)O^{16}$, with $E_p=4.025$ Mev and a target thickness of 55 kev. This spectrum shows that there are virtually no particles emitted below the intense ground-state group when they are being emitted to a sharp state. Thus the anomaly was not induced by instrumental defects. Figure 14 shows the alpha spectrum taken of $B^{11}(p,\alpha)$-$Be^8(0)$, $E_p=4.025$ Mev, with the same target used for Fig. 8 but with the target placed in its holder backwards. The purpose of this test was to ascertain that no significant amount of B^{11} was present on the *back*

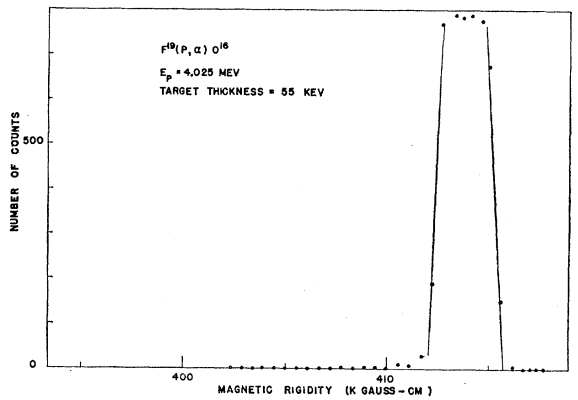

FIG. 13. Alpha-particle spectrum from $F^{19}(p,\alpha)O^{16}(0)$, with $E_p=4.025$ Mev. This experiment was performed to investigate the background in the immediate vicinity of an intense group of particles. The tail on the particle group is seen to extend over a region smaller than the width of the peak itself.

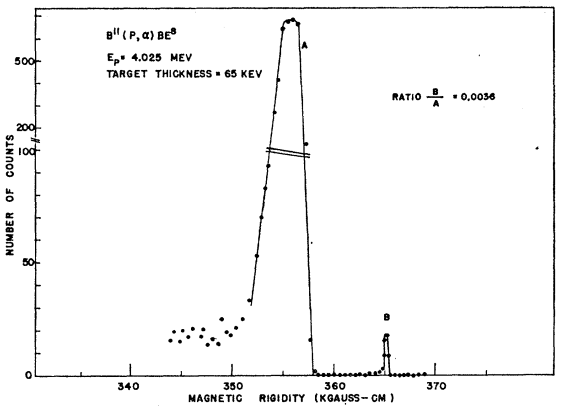

FIG. 14. Alpha-particle spectrum from $B^{11}(p,\alpha)Be^{8}(0)$, with the target used for the spectrum of Fig. 8 placed in its holder backwards. This experiment accurately measured the amount of B^{11} present on the back side of the foil on which B^{11} had been evaporated. Particle group B results from boron on the back side; particle group A results from boron on the front side.

side of the C^{12} foil. This could have resulted in a group of alpha particles in the region $E_x \sim 0.75$ Mev. Figure 14 shows that this effect was only 3.6×10^{-3} and this could account for only about 10% of the low-energy anomaly shown in Fig. 8.

The fit to the data of Figs. 7–10 is not very good for $E_x > 3$ Mev, but an extensive effort to fit this region has *not* been made. The exact shape of the 2^+ Be^8 anomaly is very sensitive to small variations in the D-wave phase shift. In addition an inclusion of ρ_4 in the calculations of the cross section might have improved the fit. However, the real interest in these experiments was in the energy region $0 \leqslant E_x \leqslant 3$ Mev, since this energy region contains the predicted spatial localization anomaly. The experiments reported in this paper confirm the existence of this anomaly. No other explanation of the anomaly is known: for example, there is very good evidence that Be^8 has no "state" in the usual sense at an energy of about 0.7 Mev. Thus it seems that the anomaly supplies indirect, but strong, evidence that in these three-body nuclear decay processes the dominant mechanism is a sequence of two-body decays.

APPENDIX

The calculation of the spectrum of the breakup group of particles was made in the following manner. Figure 15 is a diagram of the velocity vectors for the reaction

$$B^{11}+p \rightarrow Be^{8*}+\alpha_0; \quad Be^{8*} \rightarrow \alpha_1+\alpha_2.$$

Let

$$N_0 \equiv \bar{\rho}(E_x)A/V_0^2,$$

and

$$dN_{1,2} \equiv 2\bar{\rho}(E_x)\,\sin\beta d\beta d\phi \times A\,\cos\gamma/4\pi V_{1,2}^2,$$

where $V_{\text{lab}}=\alpha$-particle velocity detected by spectrometer, $V_{\text{c.m.}}$=center-of-mass velocity of C^{12*}, V_0=velocity of α_0, V_8=velocity of Be^8, $V_{1,2}$=velocity of α_1 and α_2, $\bar{\rho}(E_x)=\rho(E_x)\times$penetrability, and A=acceptance solid angle of spectrometer. N_0 represents the

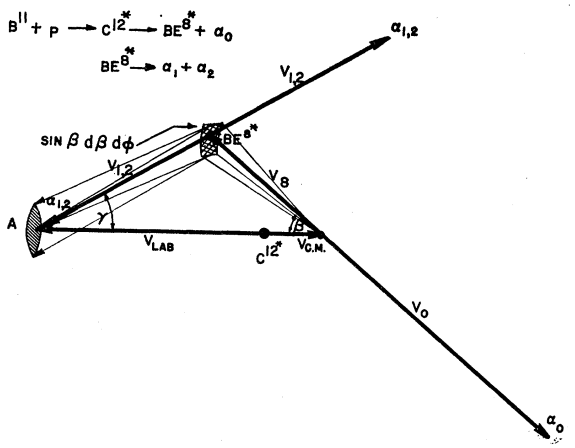

FIG. 15. Vector diagram of the velocity vectors for the reaction $B^{11}+p \rightarrow Be^{8*}+\alpha_0$; $Be^{8*} \rightarrow \alpha_1+\alpha_2$.

number of particles of type α_0 and velocity V_{lab} detected (entering A). $N_{1,2}$ represents the number of particles of type $\alpha_{1,2}$ detected, with V_{lab} determined by the values of V_8, $V_{1,2}$, and β. From the kinetics of the reaction:

$$B^{11}+p \rightarrow Be^{8*}+\alpha_0+Q_0-E_x,$$
$$Be^{8*} \rightarrow \alpha_1+\alpha_2+Q_2,$$

if follows that

$$V_8^2=[Q_0-E_x+(11/12)E_p]/12,$$
$$V_{1,2}^2=(E_x+Q_2)/4,$$

where mass of proton=1 unit, E_p=bombarding energy, E_x=energy of excitation in Be^8, and $c=V_{\text{lab}}+V_{\text{c.m.}}$. Thus

$$\sin\beta d\beta=\left[\frac{V_{1,2}^2+7V_8^2-c^2}{48cV_8^3}\right]dE_x,$$

and

$$\cos\gamma=(V_{1,2}^2+c^2-V_8^2)/2cV_{1,2},$$

$$N_{1,2}=A\frac{(48)^{\frac{1}{2}}}{96\pi}\int_{E_{x1}}^{E_{x2}}\pi\bar{\rho}\frac{[a+bE_x-(1/9c^2)E_x^2]}{[(\alpha-E_x)E_x]^{\frac{3}{2}}}dE_x,$$

where

$$a=\tfrac{2}{3}\alpha-c^2+(1/144c^2)[18\alpha Q_2-7\alpha^2+9Q_2^2],$$
$$b=2\alpha/9c^2-\tfrac{2}{3},$$
$$c^2=(V_{\text{lab}}+V_{\text{c.m.}})^2,$$
$$\alpha=Q_0+(11/12)E_p,$$

and E_{x1}=lower limit of integration, determined by the velocity V_{lab} for which $N_{1,2}$ is being integrated; E_{x2}=upper limit for which $N_{1,2}$ is being integrated.

It is possible to integrate this expression numerically for any particular value of V_{lab} and E_p. The expression was evaluated for a number of values of V_{lab} corresponding to the energies of emitted alpha particles α_0 of interest, and the result compared with the value of N_0 for the same α_0 energy. A similar calculation was performed for the $Be^9(p,\alpha)Li^{6*}$; $Li^{6*} \rightarrow \alpha+d_1$ reaction.